THE ASTROPHYSICAL JOURNAL, 464:507–515, 1996 June 10

SOLAR MODULATION OF COSMIC ELECTRONS

JOHN M. CLEM, DAVID P. CLEMENTS, JOSEPH ESPOSITO,[1] PAUL EVENSON,
DAVID HUBER, AND JACQUES L'HEUREUX
Bartol Research Institute, University of Delaware, Newark, DE 19716
PETER MEYER
Department of Physics, University of Chicago, Chicago, IL 60637
AND
CHRISTIAN CONSTANTIN
Institut für Kernphysik, Universität Kiel, 24118 Kiel, Germany
Received 1995 August 15; accepted 1995 December 27

ABSTRACT

We present new cosmic electron measurements obtained from the MEH electron experiment on the *ISEE 3/ICE* spacecraft for the period 1990 through early 1995, and we discuss these in the context of other data. Charge sign dependence of solar modulation is confirmed at energies as high as 5.8 GeV, but the major reduction of fluxes of these electrons in the 1970s does not seem to be reproduced in the current decade. We also report the first data from AESOP (Anti Electron Sub Orbital Payload), a magnet spectrometer using a ring-dipole permanent magnet and digital optical spark chambers. AESOP flew in a preliminary configuration from Lynn Lake, Canada during the summer of 1994. In this configuration the useful energy range is limited to a narrow band around 1.5 GeV, where we measured an abundance of positrons, relative to all electrons, of 0.32 ± 0.18. A consistent picture of the positron abundance and its time variation may be emerging from the world data set.

Subject headings: cosmic rays — solar-terrestrial relations — space vehicles

1. INTRODUCTION

Fluxes of cosmic-ray nuclei have now been monitored continuously with high precision for more than 40 years (Simpson, Fonger, & Treiman 1953). Measurement of electrons began nearly a decade later (Earl 1961; Meyer & Vogt 1961), but lack of a ground-based monitoring technique has resulted in a data set with much less internal consistency over time. The longest series of electron measurements was begun in 1968 at the University of Chicago (Hovestadt, Meyer, & Schmidt 1970; Schmidt 1972; Fulks 1975; Evenson et al. 1979) and has continued at Bartol Research Institute since 1984 (Tuska 1990; Tuska, Evenson, & Meyer 1991; Evenson et al. 1995) using the balloon-borne detector LEE (Low Energy Electron). In the remainder of this paper, these data will be referred to collectively as the "LEE Series."

The second longest series of electron measurements is now concluding as, due to reduced spacecraft power capacity, the MEH instrument (Meyer & Evenson 1978) on *ISEE 3/ICE* must be turned off by 1996 March, after operating continuously since 1978 August 14. We present data obtained through the end of 1994 from the MEH instrument as well as the first data from our new instrument AESOP (Anti-Electron Sub Orbital Payload). AESOP is designed to have similar energy response to LEE, but in addition it resolves positrons and negatrons separately. We have proposed to replace LEE with AESOP in the continuing series of balloon measurements.

Solar modulation is a complex process with major dependences on rigidity, particle species, and charge sign. We are only beginning collaborative efforts to secure data needed for a full analysis of the relative modulation of electrons and nuclei. Here we limit ourselves to the conclusions that we can be drawn from the electron data, supplemented by neutron monitor observations. We use these data to construct a phenomenological characterization of the charge sign dependence of solar modulation. We argue that, although the errors are still large, a consistent picture seems to be emerging regarding the relative positron abundance and its change with time. Our main conclusion is that over the energy range from 0.5 to 20 GeV, positron abundances are consistent with a secondary origin in a relatively standard leaky box picture of galactic confinement. Particularly below 5 GeV, incomplete understanding of the charge sign dependence of modulation makes quantitative comparison of data with calculations impossible.

2. TOTAL ELECTRON FLUXES

We first present an extension of the work of Tuska (1990) and Tuska et al. (1991) with the University of Chicago electron instrument (Meyer & Evenson 1978), on the *ISEE 3/ICE* spacecraft. Minimum ionizing particle signals in the outermost silicon detector showed a sharp decrease in 1989 October, following an intense interplanetary particle event. Despite an initial recovery, the detector has had a persistent degradation in signal over time so that by late 1994 the position of the singly minimum ionizing peak had fallen to 80% of its value before the event. Analysis of other detectors showed smaller calibration shifts.

Therefore, we developed a process to correct the detector signals by applying multiplicative factors in the data analysis. The correction factors were obtained by observing minimum ionizing peaks in each detector over time and dividing these peak positions into a reference value derived from the average peak position early in the mission. The resulting time-dependent correction can be applied on an event-by-event basis over the span of the mission. We have also confirmed the validity of the model of Tuska (1990) to

[1] Present address: USRA, Goddard Space Flight Center, Code 662, Greenbelt, MD 20771.

correct the assumed efficiency of the gas Cerenkov detector for gas loss. The new correction procedure has been applied to all the data reported in this paper. In addition, we average over Carrington rotations rather than arbitrary 27 day intervals beginning on the first day of the flight. As a consequence, data reported here may appear slightly different from earlier presentations of the same data. We have, however, found no case in which the difference exceeds the stated errors on the measurements.

Figure 1 presents an overview of the time history of solar modulation. The Climax neutron monitor shown in the top panel provides the longest record of high-accuracy data on cosmic-ray nuclei. For purposes of discussion, the data may be taken to represent the flux of (positively charged) protons at a mean rigidity of 10.7 GV. Various time points discussed in this paper are indicated by letters in Figure 1, as is the solar polarity state. As we discuss in some detail later, heliospheric modulation is known to depend upon the sign of the particle's charge and must affect e^+ and e^- differently. This knowledge comes from observations of the effect of the orientation of the solar magnetic field on cosmic-ray fluxes. Although the Sun has a complex magnetic field, the dipole term nearly always dominates in determining the magnetic field of the solar wind. The projection of this dipole on the solar rotation axis (A) can be either positive, which we refer to as the A^+ state, or negative, which we refer to as the A^- state. At each sunspot maximum, the dipole reverses direction, leading to alternating magnetic polarity in successive solar cycles. This reversal is better viewed as a collapse and regeneration, rather than a rotation.

The solar polarity reversals shown in Figure 1 are the result of magnetogram observations taken over the last four solar cycles (Babcock 1959; Howard 1974; Webb, Davis, & McIntosh 1984; Lin, Varsik, & Zirin 1994). The symbols "N" and "S" in Figure 1 signify the best times, according to these observations, as to when these polar regions reversed polarity. Babcock (1959) was the first to observe a change in the polarity state when he observed the northern (southern) polar region change to positive (negative) polarity, i.e., to an A^+ state. The polarity reversals shown are for heliographic latitudes greater than 70°, except for Babcock (1959), which covers 80°–50° latitude in each hemisphere.

In the bottom panel we show our new data, together with a compilation of earlier measurements of the electron flux, at an energy of approximately 1.2 GeV. We have displayed data at this energy because it is probably the cleanest energy to observe, and therefore it should provide the best reference for the discussion of electron modulation. There are several reasons why electrons of this energy are comparatively easy to observe. Most importantly, the primary spectrum is typically rather flat at this energy, so errors in energy calibration and finite energy resolution of detectors are minimized. Further, showers produced in calorimeters are well developed and easily separated from the signal of noninteracting high-energy protons, while the total number of showers produced by proton interaction is still small compared to the electron flux. At balloon float altitude, primary electrons at this energy typically dominate atmospheric secondaries. Finally, for launches in northern Canada, return albedo electrons which cloud the picture at lower energies have never been observed at energies this high.

Our data confirm that charge sign dependence of solar

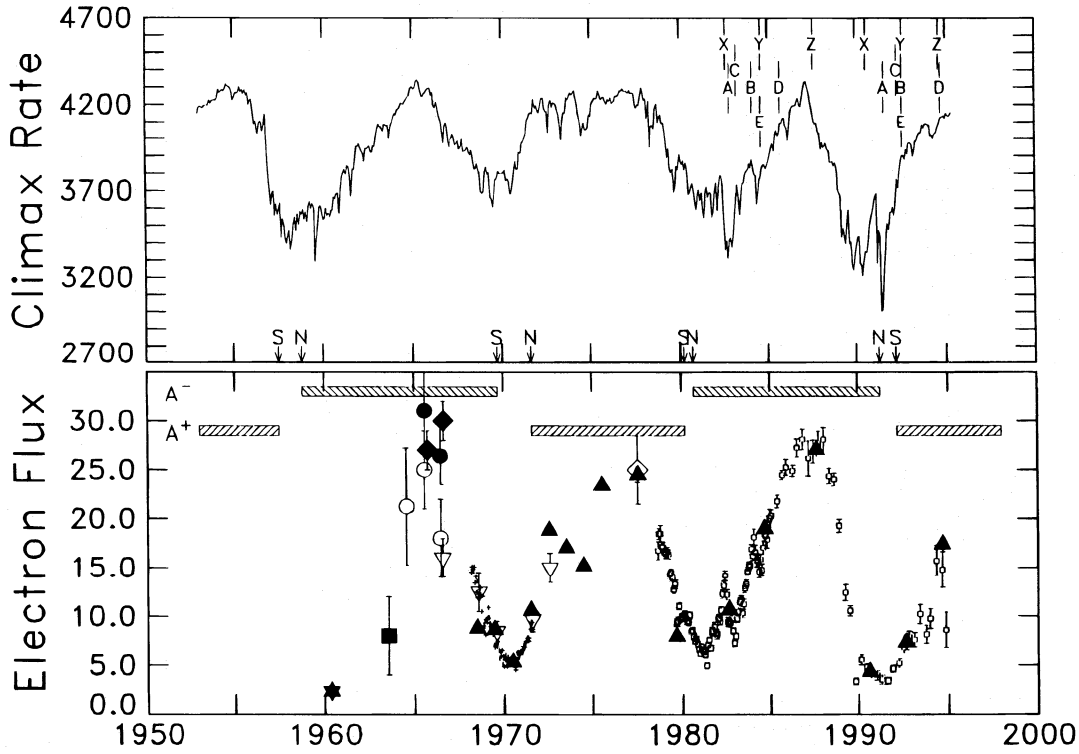

FIG. 1.—Summary of measurements of solar modulations. *Top:* Carrington rotation averages of the Climax neutron monitor (response approximately 10.7 GV). *Bottom:* Electrons with energy approximately 1.2 GeV. Balloon data (*large symbols*) sources are as follows: *star*, Earl (1961); *filled square*, Freier & Waddington (1965); *open circles*, L'Heureux & Meyer (1968); *filled circles*, Fanselow et al. (1969); *filled diamonds*, Bleeker et al. (1968); *open triangles*, Rockstroh & Webber (1969), Webber, Kish, & Rockstroh (1973); *filled triangles*, LEE Series; *open diamond*, Bland (1979). Spacecraft data (*small symbols*) sources are as follows: *crosses*, *OGO 5* (Burger & Swanenburg 1973); *open squares*, *ISEE 3/ICE*. Other notes and symbols are described in the text.

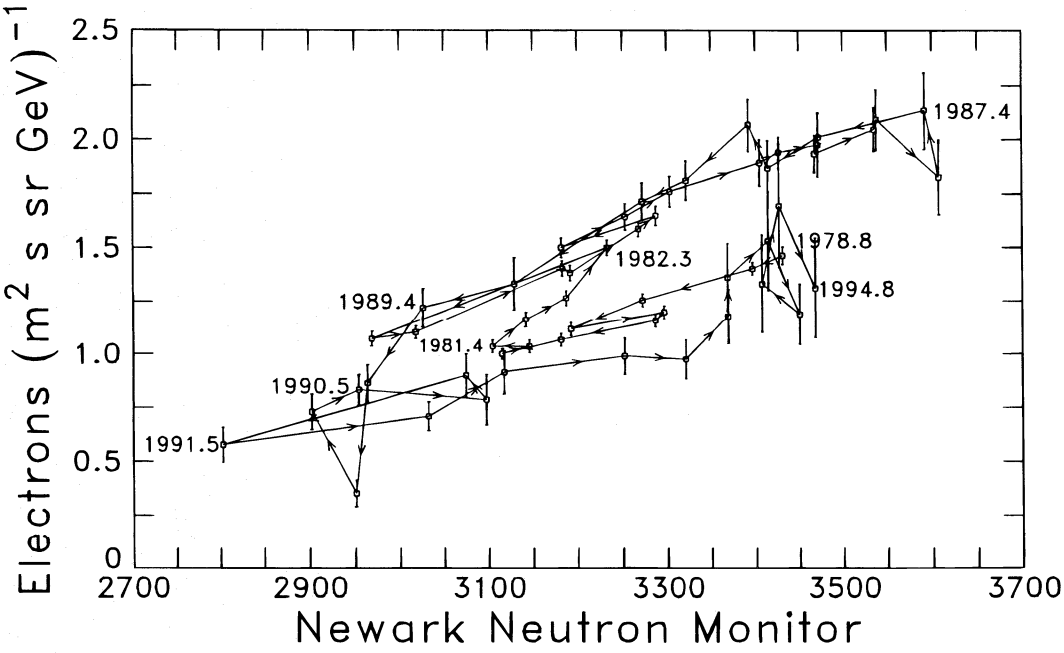

FIG. 2.—Electrons with mean energy of 5.8 GeV measured by *ICE* plotted against the counting rate of the Newark neutron monitor for the time period 1978–1994.

modulation extends to energies as high as 5.8 GeV. Figure 2 shows the flux of electrons with mean energy of 5.8 GeV measured by *ICE* plotted against the counting rate of the Newark neutron monitor for the time period 1978–1994. The measurements in the 1990s follow the trajectory defined in the late 1970s, showing significantly lower electron fluxes at corresponding neutron monitor levels than in the 1980s. Separate trajectories for the two polarity states are well defined at this high energy and at lower energy (Garcia-Munoz et al. 1986, 1991) but the transition between the two states does not occur simultaneously at all energies (Ferrando et al. 1995; Rastoin et al. 1996). Further, the magnitude of the apparent charge sign dependence visible in Figure 2 is much less than the difference in electron fluxes reported by Tuska et al. (1991) comparing the mid-1970s to the mid-1980s.

A more specific characterization of the observations in the 1970s is emerging. One might now best describe the situation as a suppression of high-energy electron fluxes in the 1970s relative both to the neutron monitor and to lower energy electrons. The behavior within the electron spectrum is illustrated in Figure 3, where the left panel shows the relative fluxes of 1.2 and 5.8 GeV electrons over the course of the *ICE* mission. While the relationship is neither perfect nor linear, there is no indication of any dependence on solar polarity state. Such a dependence would not be expected for

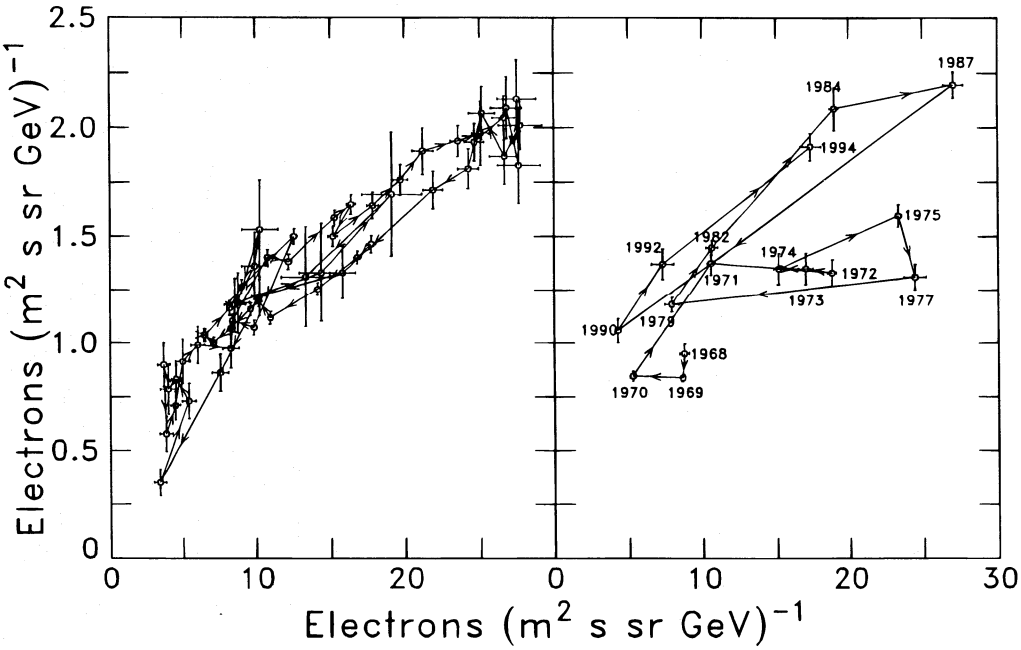

FIG. 3.—Flux of 5.8 GeV electrons plotted against flux of 1.2 GeV electrons. *Left:* Measurements from *ICE* 1978–1994. *Right:* Measurements from the LEE balloon instrument 1968–1994.

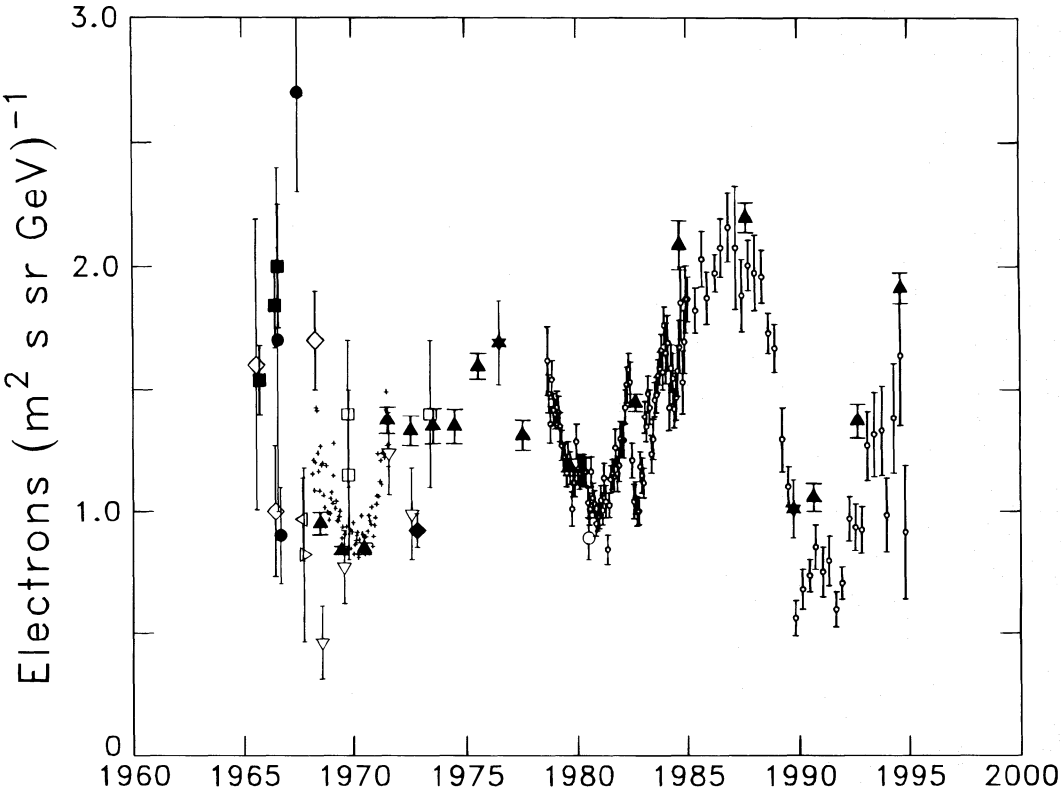

FIG. 4.—Compiled measurements of electrons at an approximate mean energy of 5.8 GeV. Balloon data (*large symbols*) sources are as follows: *open diamonds*, Fanselow et al. (1969, 1971); *filled squares*, Bleeker et al. (1968); *filled circles*, Earl, Neely, & Rygg (1972); *left arrowhead*, Marar, Freier, & Waddington (1971); *right arrowed*, Oran, Frye, & Wang (1969); *filled triangles*, LEE Series; *open triangles*, Rockstroh & Webber (1969), Webber et al. (1973); *open squares*, Meegan & Earl (1975); *stars*, Golden et al. (1994); *open circle*, Tang (1984). Spacecraft data (*small symbols*) sources are as follows: *crosses*, *OGO 5* (Burger & Swanenburg 1973); *open squares*, *ISEE 3/ICE*.

particles of the same charge sign. Where coverage overlaps in time, the same correlation appears in data from the LEE series as shown in the right panel. However, the time period from 1972 to 1977 now stands out with respect both the the opposite polarity 1980s, and to the same polarity 1990s. Measured electron fluxes at 5.8 GeV in the 1970s are systematically low.

As we have pointed out repeatedly (Evenson et al. 1995), the lack of a comprehensive, confirming measurement during this time interval is disturbing. Figure 4 shows a compilation of published measurements of the electron flux at approximately 5.8 GeV. There is no evidence that electron fluxes in the 1970s ever reached the levels measured in the 1980s. Assuming that the measurements are correct, it is difficult to see how such behavior within the electron spectrum could be a direct manifestation of charge sign dependence. This supports the conclusion of Tuska et al. (1991) that the explanation must be sought in some other aspect of the modulation process. Specifically, they proposed that the high energy density of the anomalous component in the outer heliosphere might provide a distant linkage to charge sign. Whatever the process, it does not seem to be operating in the present solar cycle.

With this in mind, we believe that the comparison of data between the 1980s and 1990s is the best way to investigate the inherent charge sign dependence of solar modulation. To characterize the energy dependence of this phenomenon, we have selected pairs of time intervals to have similar (for each pair) neutron monitor level but opposite solar magnetic polarity. In Figure 5 the ratio of the electron flux in the A^+ polarity state to that in the A^- state determined for each pair of intervals is plotted as a function of energy. Time intervals chosen for this analysis are indicated in Figure 1 by letters. Symbols A–E indicate *ISEE 3/ICE* electron measurements averaged over three Carrington rotations centered on the plotting symbol. Symbols X–Z indicate LEE balloon flights. Time intervals A–D were selected to have nearly the same neutron monitor level, X–Z were selected to be as close in neutron monitor level as possible given the

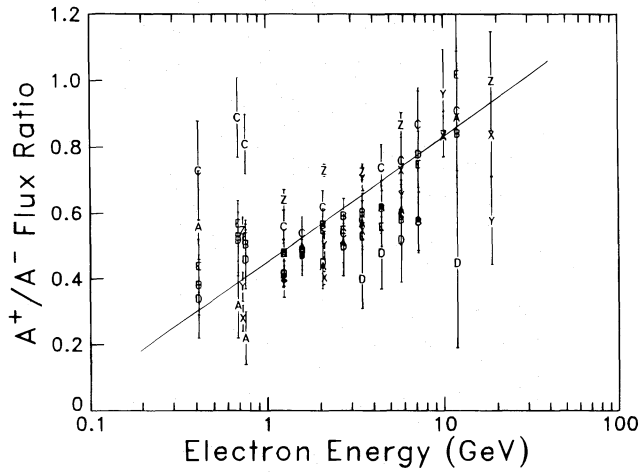

FIG. 5.—Energy dependence of the charge sign effect in modulation. Solid line is a least-squares fit to the data. See text for explanation of plotting symbols.

discrete flight dates, while for comparison the symbol E refers to *ISEE 3/ICE* measurements centered on the time of the LEE flights corresponding to symbol Y.

Although there is considerable scatter to the data, the overall organization is quite pronounced. Because of the way the data have been presented, the ratio must approach 1 at high energy as modulation itself disappears. Charge sign dependence appears to be present at all energies, possibly even having a larger relative effect at the higher energies than the lower. For later use in our discussion of the positron abundance, we show also a least-squares straight-line fit to the ratio as a function of logarithm of energy.

3. POSITRONS AND NEGATRONS

In Figure 6 we present a compilation of published data on the positron abundance. In preparing Figure 6, we have excluded data in which the reported positron flux has 1 σ errors that include zero, and we have excluded integral points. We have also excluded measurements that are not demonstrably free of atmospheric return albedo contamination. Early determinations at low energy in particular were published before the time-dependent nature of this source of contamination was established (Jokipii, L'Heureux, & Meyer 1967). Also shown in Figure 6 is a measurement obtained in 1994 from the new payload (AESOP) being developed at Bartol. We give details of the instrument, flight, and data analysis in an appendix.

To focus our discussion, we consider a very simple model for charge sign–dependent solar modulation:

$$f_{\rm E}(P, \phi, qA) = C(q{\rm A}, P) \times M(P, \phi) \times f(P) . \quad (1)$$

This model assumes that the flux at Earth, $f_{\rm E}$, of a particle species as a function of rigidity, P, charge sign, q, solar magnetic polarity, A, and phase of the solar cycle, ϕ, is determined by the product of the interstellar flux, $f(P)$, and two modulation factors. This formalism ignores adiabatic deceleration but is consistent with the early phenomenological treatment of modulation. In this model, ϕ represents solar (or sunspot) cycle phase in a very general sense, but we have chosen the symbol deliberately to call to mind an association with modulation level. One modulation factor depends on rigidity and phase and corresponds to the classical modulation factor. The other factor may also depend on rigidity but carries the entire dependence on charge sign. We assume further that this dependence is only on the product qA and that q and A each assume only the values ± 1.

Now let n represent the interstellar flux of negatrons and p represent the interstellar flux of positrons. The conventional way of presenting the positron abundance is the ratio of positrons to total electrons, denoted F when measured in interstellar space:

$$F(P) = \frac{p(P)}{p(P) + n(P)} . \quad (2)$$

Because of our assumptions, the corresponding quantity at Earth, $F_{\rm E}$, is independent of ϕ:

$$F_{\rm E}(A, P) = \frac{p(P)C(A, P)}{p(P)C(A, P) + n(P)C(-A, P)} . \quad (3)$$

We can also express the ratio (observed at Earth) of total electron fluxes in the A^+ cycle to total electron fluxes at a similar phase in the A^- cycle:

$$R(P) = \frac{p(P)C(A, P) + n(P)C(-A, P)}{p(P)C(-A, P) + n(P)C(A, P)} . \quad (4)$$

In our simple model, the solar cycle phase is not present in this expression either. One should, in fact, view the lack

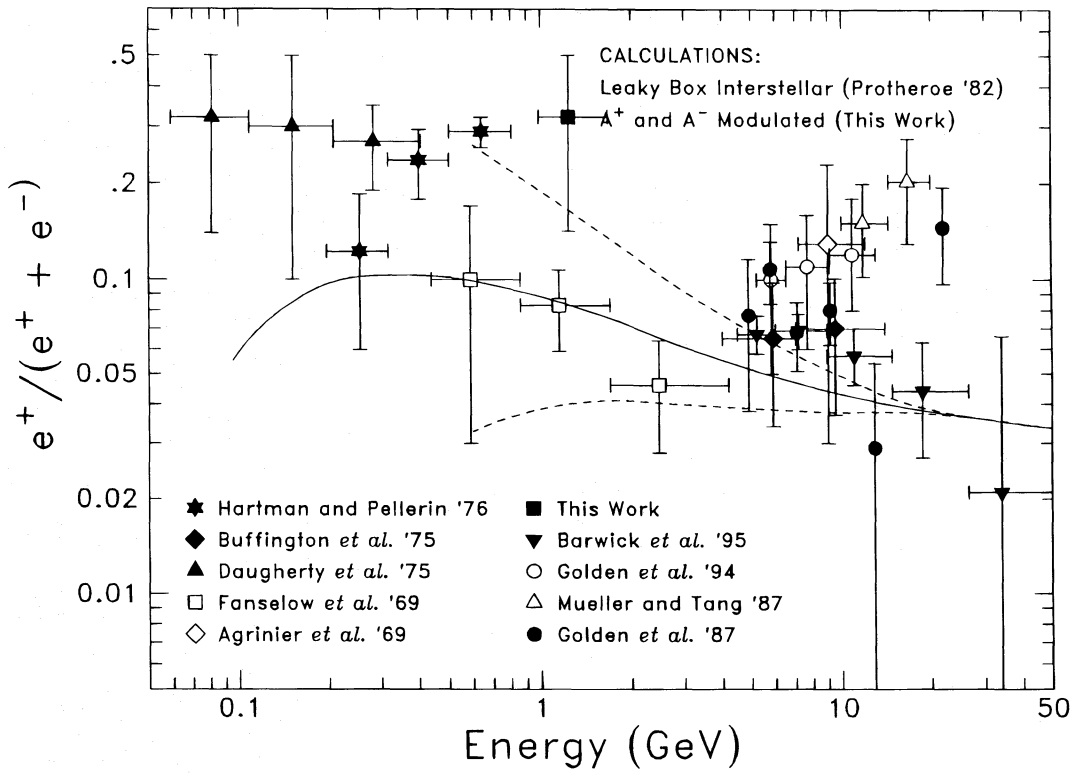

FIG. 6.—Compiled measurements and calculations of the positron fraction as a function of energy during different epochs of solar magnetic polarity. Solid symbols and upper dashed line represent A^+ state. Open symbols and lower dashed line represent A^- state.

of dependence on solar cycle phase in the data presented in Figure 5 as the principal justification of our use of this simple model. While these equations cannot be solved for all the modulation factors, they can be manipulated by elementary mathematics to yield a prediction for the observed positron fraction at Earth in terms of F and R. As an example, the result for the A^+ state and a particular rigidity is

$$F_E = \frac{F^2(R+1) - F}{R(2F-1)} . \quad (5)$$

By taking the fit line in Figure 5 to represent $R(P)$ and the Protheroe calculation for $F(P)$, one obtains the dashed curves in Figure 6. Since Protheroe (1982) considered modulation, but not charge sign–dependent modulation, we have simply taken the quantity he calculated as the interstellar value. This is consistent with our assumption that the factor M in equation (1) is the same for positrons and negatrons. The upper curve in Figure 6 is for the A^+ magnetic state, and the lower curve is for the A^- magnetic state. The calculation is only shown for the energy range covered by the data in Figure 5.

Our analysis is similar to that of Moraal, Jokipii, & Mewaldt (1991) in some respects. It differs in that they use a model to estimate the charge sign dependence, while we estimate it phenomenologically from data in alternate polarity states. They display their results by adjusting data points, while we present modified calculations. For the present, the key conclusion to draw seems to be that the rather large amount of charge sign dependence observed is not outside the range attainable in calculations.

4. DISCUSSION

There is rather good agreement of the A^+ measurements (Fig. 6, *solid symbols*) with the A^+ calculation. The recent measurements of Barwick et al. (1995) track the predicted abundance quite closely and are consistent with earlier determinations. Our new measurement, even with its large errors, confirms the Hartman & Pellerin (1976) observation of a large positron abundance in the midrange energies. Only the highest energy point of Golden et al. (1987) deviates significantly from the pattern. This measurement is contradicted by the Barwick et al. (1995) result and if taken literally implies a rather unlikely energy dependence compared to the next point from the same experiment.

Fewer measurements in the A^- state have been made. In the few GeV energy range, only one A^- measurement appears (Fanselow et al. 1969). The reported ratios are significantly lower than those from the A^+ measurements, and the difference is consistent with the prediction. In contrast, at 15 GeV the Müller & Tang (1987) determination cannot be reconciled with the Barwick et al. (1995) results by invoking charge sign dependence. A factor of 5 change in the flux of a cosmic-ray species at 15 GeV due to solar modulation, where typical modulation amplitudes would be 10% at most, is not supported by any other data. But at energies around 10 GeV, the Agrinier et al. (1969), Müller & Tang (1987), and Golden et al. (1994) measurements show a curious consistency. Even with the large errors, as a group these measurements are clearly higher than those in the A^+ set, and no individual measurement disagrees with the pattern of solar polarity ordering outside its assigned error. The required charge sign dependence (less than a factor of 2) is at least roughly comparable to the observed modulation amplitude of the Climax neutron monitor (see Fig. 1). Depending on how one views the errors, and whether one believes that there is an energy dependence, the magnitude of the splitting is not too different from the prediction, only the direction is wrong. A reversal in direction of the charge sign dependence at a particular energy is in fact possible. The mechanism proposed by Bieber, Evenson, & Matthaeus (1987) actually predicts such a reversal at rigidities at which particle gyral radii are comparable to the plasma correlation length, which is approximately 10 GV near Earth.

On the negative side, there is no indication in Figure 5 of any strange behavior of the total electron fluxes near 10 GeV, although statistics are admittedly poor. Also, the A^+ observations in Figure 6 follow the A^+ prediction, so the implication would be a positron flux higher than that calculated by Protheroe (1982). Finally, from neutron monitor data it is clear that there are distortions in the spectral shape of positive particles (Moraal et al. 1989; Popielawska & Simpson 1990), but these distortions seem small compared to what might be expected from a reversal of the direction of charge sign dependence. This point might be regarded as conclusive except for the possibility raised from the study of the 5.8 GeV electrons that the electrons and nuclei may be subject to significantly different modulation not directly related to charge sign.

Perhaps our most important conclusion is that an astrophysical interpretation of positron abundances requires not only more accurate measurements but a full understanding of the solar magnetic influence before anything like quantitative comparisons with models can be made. Some of this might come from a careful consideration of data on the modulation of nuclei, but the definitive work can be done only with repeated positron observations. Of course, the cosmic-ray antiproton abundance relative to protons will be similarly uninterpretable without this understanding.

We thank Leo Krawczyk for his assistance in the reduction of the *ISEE 3/ICE* data. With the exception of the magnet (procured from Field Effects, Inc.) and the flight shell (kindly loaned to us by Peter Meyer), AESOP was built entirely in the Bartol Research Institute—Department of Physics and Astronomy shops at the University of Delaware. We thank in particular Andrew McDermott, Gerald Poirier, Tom Reed, Tom Reilly, and Len Shulman for their effort and support. We also thank Randy Jokipii, Vernon Jones, Horst Kunow, Karen Magee-Sauer, John Petrakis, Dave Seckel, Evelyn Tuska Patterson, and Gerd Wibberenz for many useful discussions. Miriam Forman has been a particular friend of this effort over the years and was a welcome and useful participant in the 1992 engineering flight campaign. Part of this work was performed while P. E. was in residence at the University of Kiel with the support of an Alexander von Humbolt Foundation Senior Research Award. This work was supported by in part by NASA grant NAG 5-2606 and by NSF grants ATM 91-15492, OPP-9219761, and ATM-9314683. Construction of AESOP was funded primarily by NASA under grant NAG 5-1040. Launch services were provided by NASA through the National Scientific Balloon Facility. Climax data were obtained from the University of Chicago, supported by NSF grant ATM-9420790.

APPENDIX

August of 1994 marked the first scientific flight of the Anti Electron Sub Orbital Payload (AESOP) from Lynn Lake, Manitoba. Clem et al. (1995a, b) discuss the construction and calibration of AESOP. The 1994 flight involved a preliminary version of the instrument with a high restricted energy range, so we are deferring a full publication of our results until a flight of the final configuration takes place. This is expected in 1996. Since the 1994 flight yielded a measurement consistent with the rather high positron abundance found by Hartman & Pellerin (1976), we include a brief discussion of the instrument and this measurement in the present paper.

A schematic diagram of the AESOP instrument as flown is shown in Figure 7. The instrument consists of six 1 cm thick circular NE-102A plastic scintillators (T1–T4, A1–A2), a 41.5 g cm^{-2} lead-glass calorimeter (Lead Glass), and four spark chamber tracking modules (SC1–SC4). The AESOP magnet, mounted between SC2 and SC3, is a rare Earth (Nd-Fe-B) ring-dipole with a typical field-integral of 90 kG cm^{-1}. For the 1994 flight, the instrument geometry was defined by T1, T3, A1, and A2, plus a variable threshold on the calorimeter. Using the bottom of the calorimeter as the defining aperture, the geometry factor was 8.7 cm^2 sr. The full 40 cm^2 sr geometry factor of the magnet spectrometer will be exploited in future enhancements to the instrument. The lead-glass calorimeter is a cylinder of Schott SF-5 lead glass that serves both to produce an electromagnetic cascade and to measure the energy deposited through the production of Cerenkov radiation. The calorimeter is viewed by three Hamamatsu R329 photomultiplier tubes. A 1 cm thick lead slab allows T3 to observe the initial stage of shower development, while T4 counts the particles emerging from the lead glass.

The AESOP spark chambers, developed at the Bartol Research Institute, have four gaps bounded by 13 μm thick stretched aluminium foil plates. Two front-surfaced mirrors are mounted on the inside of the rear chamber walls, resulting in three images of a spark to provide overdetermined spatial information. The horizontal positions of the spark images are digitized using standard 35 mm camera lenses (28 mm focal length) and linear charge-coupled device (CCD) arrays containing 3456 10.7 × 10.7 μm elements. Each chamber gap is viewed by an individual camera (Clements et al. 1991). Before installing the plates defining the spark gaps, the chambers were calibrated (Clements 1991; Clements & Evenson 1993; Constantin 1995) using a rotary table to move a 3 mm wide neon bulb in the fiducial volume. The rotary table moves the bulb around a precise circle in equal angular intervals. A nonlinear fit to the calibration data determines various parameters that characterize the optical system. Typically, the circle reconstruction residuals in the x-plane are 30 μm, while in the y-plane they are 70 μm.

The final configuration of AESOP will include a gas Cerenkov detector, but construction of this expensive element has been deferred until operation of the novel design hodoscopes could be proven. Without the Cerenkov, the useful energy range of AESOP is limited and would ordinarily not justify the expense of a balloon flight. However, we took advantage of an opportunity to fly AESOP on the same balloon that carried the LEE instrument (Hovestadt et al. 1970) on its 1994 flight. At energies below 1 GeV, an accurate measurement of a flux versus altitude profile is needed to allow subtraction of atmospheric secondary contamination. While positrons could be separated cleanly from protons if the data could be returned, the background event rate without the Cerenkov detector would result in unacceptable dead time of the instrument. As the balloon rose, a discriminator on the calorimeter was therefore varied to control the counting rate of the instrument. Above

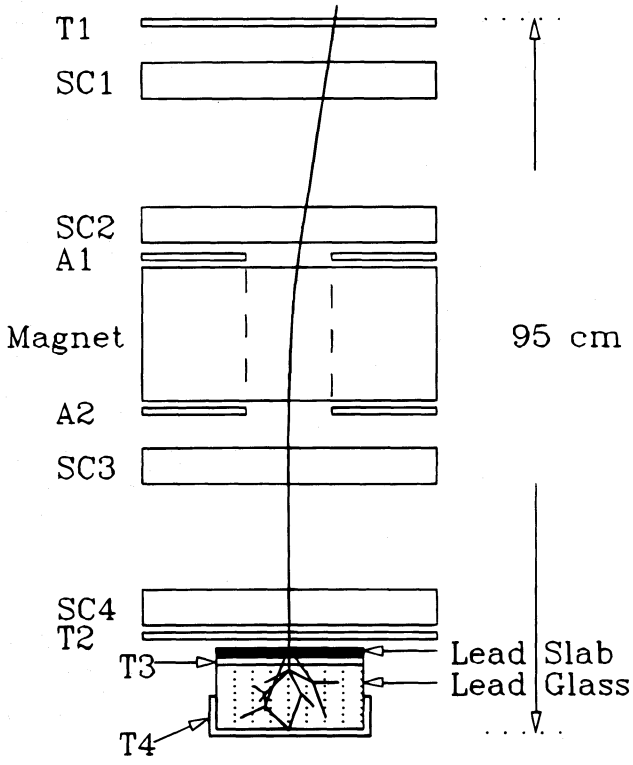

FIG. 7.—Block diagram of the AESOP instrument showing the preliminary configuration flown in 1994.

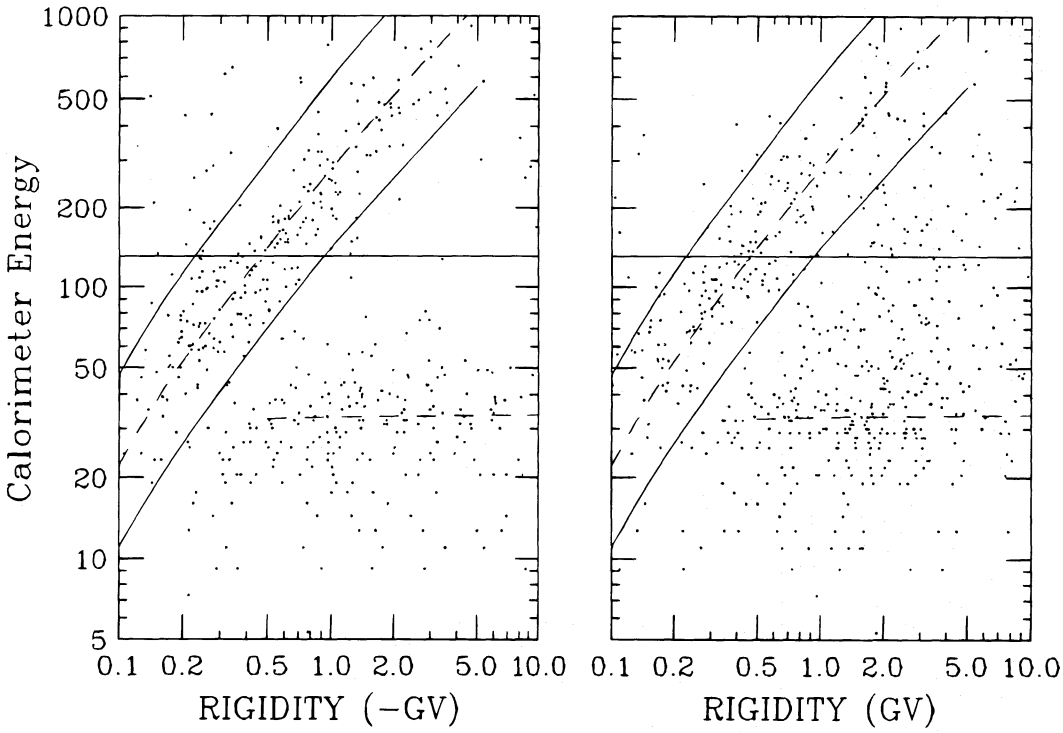

FIG. 8.—Energy deposit in the AESOP lead glass calorimeter (arbitrary units) plotted against rigidity measured by the magnet spectrometer. Lines are explained in text.

about 2 GeV, a proton can deposit enough energy in the calorimeter to mimic a positron of the same rigidity, hence the Cerenkov is needed in a different role for the upper energy range of the instrument. At intermediate energies, protons do not carry enough kinetic energy to mimic positrons of the same rigidity, and a less accurate measurement of the atmospheric growth curve can be tolerated, since the eventual correction is smaller.

In Figure 8 we show data obtained on the 1994 flight as scatter plots of calorimeter signal against measured rigidity. The dashed lines in Figure 8 show the results of a GEANT (CERN ASD Group 1994) simulation of the position of the muon track (horizontal lines) and the positron and negatron tracks (diagonal lines). The muons were recorded during an interval of 2 hours on the ground before flight. During flight, the discriminator level was varied, but it was always high enough so that the instrument was not triggered by singly charged, noninteracting particles. We show data taken on the ascent up to a pressure altitude of 5.5 mm of mercury. Unfortunately, at that point an electronic breakdown made further data analysis impossible.

Outside the electron track, the negative rigidity region is quite clear of background while the positive rigidities show the expected spray of interactions from the numerous protons. Nevertheless, there is a distinct gap between the proton spray and the positron track. Solid lines show cuts that were developed for scientific analysis of the data. The horizontal line represents the highest energy at which the hardware threshold on the calorimeter was placed, while the diagonal lines were chosen with the aid of the GEANT simulations to define a region that includes most of the electrons. Measured rigidity in the spectrometer was used to sort the particles into energy bins that correspond exactly to those used for the LEE analysis (Fulks 1975; Evenson et al. 1979). Events were also grouped into the same time intervals (corresponding to different altitudes) used for analysis of the 1994 LEE data (Evenson et al. 1995). Enough events for statistically significant analysis were obtained for total electrons in the 1240, 2110, and 3475 MeV energy bins, and positrons in the 1240 and 2110 MeV bins. Fluxes of total electrons (positrons plus negatrons) and identified positrons at different atmospheric depths were processed through the programs used for LEE (Fulks 1975) to deduce the primary fluxes corrected to the top of the atmosphere. Briefly, this technique uses the spectra of Daniel & Stephens (1974) of electrons at different depths in the atmosphere, fitted to the flight data, to estimate the atmospheric background and correct the observations to the top of the atmosphere. Implicit assumptions in our application of this analysis are that positron and negatron secondaries have similar dependence on atmospheric depth, and that positron and negatron primaries have similar spectra. Ultimately, the statistical limitations of the short flight make a more subtle analysis meaningless. Simulations using GEANT show that significant proton contamination of positron fluxed may occur above the 1240 MeV bin, so we report a positron abundance only for that energy.

REFERENCES

Agrinier, B., Koechlin Y., Parlier, B., Paul, J., Vasseur, J., Boella, G., Dilworth, C., Scarsi, L., Sironi, G., & Russo, A. 1969, Nuovo Cimento, 1, 53

Babcock, H. D. 1959, ApJ, 130, 364

Barwick, S. W., et al. 1995, Phys. Rev. Lett., 75, 390

Bieber, J., Evenson, P., & Matthaeus, W. 1987, Geophys. Res. Lett., 14, 864

Bland, C. J. 1979, Proc. 16th Int. Cosmic-Ray Conf. (Kyoto), 1, 467

Bleeker, J. A. M., Burger, J. J., Deerenberg, A. J. M., Scheepmaker, A., Swanenburg, B. N., & Tanaka, Y. 1968, Canadian J. Phys., 46, S522

Buffington, A., Orth, C. D., & Smoot, G. F. 1975, ApJ, 199, 669

Burger, J. J., & Swanenburg, B. N. 1973, J. Geophys. Res., 78, 292

CERN ASD Group 1984, GEANT Detector Description and Simulation Tool (CERN Program Library, Long Writeup W5013)

Clem, J. M., Clements D. P., Constantin, C., Esposito, J., Evenson P. A., Huber, D., & H'eureux J. 1995a, Proc. 24th Int. Cosmic-Ray Conf. (Rome), 3, 5

———. 1995b, Proc. 24th Int. Cosmic-Ray Conf. (Rome), 4, 1279

Clements, D. P. 1991, Master thesis, Univ. Delaware

Clements, D. P., & Evenson, P. A. 1993, Proc. 23d Int. Cosmic-Ray Conf. (Calgary), 2, 556
Clements, D. P., et al. 1991, Proc. 22d Int. Cosmic-Ray Conf. (Dublin), 2, 571
Constantin, C. 1995, Diplomarbeit, Christian Albrechts Universität zu Kiel
Daniel, R. R., & Stephens S. A. 1974, Rev. Geophys. Space Phys., 12, 233
Daugherty, J. K., Hartman, R. C., & Schmidt, P. J. 1975, ApJ, 198, 493
Earl, J. A. 1961, Phys. Rev. Lett., 6, 125
Earl, J. A., Neely, D. E., & Rygg, T. A. 1972, J. Geophys. Res., 77, 1087
Evenson, P., Caldwell, J., Jordan, S., & Meyer, P. 1979, J. Geophys. Res., 84, 5361
Evenson, P., Huber, D., Patterson, E., Esposito, J., Clements, D., & Clem, J. 1995, J. Geophys. Res., 100, 7873
Fanselow, J. L., Hartman, R. C., Hildebrand, R. H., & Meyer, P. 1969, ApJ, 158, 771
Fanselow, J. L., Hartman, R. C., Meyer, P., & Schmidt, P. J. 1971, Ap&SS, 14, 301
Ferrando, P., et al. 1995, Proc. 24th Int. Cosmic-Ray Conf. (Rome), 4, 752
Freier, P. S., & Waddington C. J. 1965, J. Geophys. Res., 70, 5753
Fulks, G. J. 1975, J. Geophys. Res., 80, 1701
Garcia-Munoz, M., Meyer, P., Pyle, K. R., Simpson, J. A., & Evenson, P. 1986, J. Geophys. Res., 91, 2858
Garcia-Munoz, M., Meyer, P., Pyle, K. R., Simpson, J. A., Evenson, P., Esposito, J., & Tuska, E. 1991, Proc. 22d Int. Cosmic-Ray Conf. (Dublin), 3, 497
Golden, R. L., et al. 1994, ApJ, 436, 769
Golden, R. L., Stephens, S. A., Mauger, B. G., Badhwar, G. D., Daniel, R. R., Horan, S., Lacy, J. L., & Zipse, J. E. 1987, A&A, 188, 145
Hartman, R. C., & Pellerin, C. J. 1976, ApJ, 204, 927
Hovestadt, D. P., Meyer, P., & Schmidt, P. J. 1970, Nucl. Instrum. Methods Phys. Res., 85, 93
Howard, R. 1974, Sol. Phys., 38, 283
Jokipii, J. R., L'Heureux, J. J., & Meyer, P. 1967, J. Geophys. Res., 72, 4375
L'Heureux, J., & Meyer, P. 1968, Canadian J. Phys., 46, S892
Lin, H., Varsik, J., & Zirin, H. 1994, Sol. Phys., 155, 243
Marar, T. M. K., Freier, P. S., & Waddington, C. J. 1971, J. Geophys. Res., 76, 1625
Meegan, C. A., & Earl, J. A. 1975, ApJ, 197, 219
Meyer, P., & Evenson, P. 1978, IEEE Trans. Geosci. Electron., GE-16, 180
Meyer, P., & Vogt, R. 1961, Phys. Rev. Lett., 6, 193
Moraal, H., Jokipii, J. R., & Mewaldt, R. A. 1991, ApJ, 367, 191
Moraal, H., Potgieter, M. S., Stoker, P. H., & van der Walt, A. J. 1989, J. Geophys. Res., 94, 1459
Müller, D., & Tang, K. K. 1987, ApJ, 312, 183
Oran, W. A., Frye, G. M., Jr., & Wang, C. P. 1969, J. Geophys. Res., 74, 53
Popielawska, B., & Simpson, J. A. 1990, in Physics of the Outer Heliosphere, ed. S. Grzeszielski & D. E. Page (Oxford: Pergamon), 133
Protheroe, R. 1982, ApJ, 245, 391
Rastoin, C., et al. 1996, A&A, in press
Rockstroh, J., & Weber W. R. 1969, J. Geophys. Res., 74, 5041
Schmidt, P. J. 1972, J. Geophys. Res., 77, 3295
Simpson, J. A., Fonger, W., & Treiman, S. B. 1953, Phys. Rev., 90, 934
Tang, K.-K. 1984, ApJ, 278, 881
Tuska, E. B. 1990, Ph.D. thesis, Univ. Delaware
Tuska, E. B., Evenson, P., & Meyer, P. 1991, ApJ, 373, L27
Webb, D. F., Davis, J. M., & McIntosh, P. S. 1984, Sol. Phys., 92, 109
Webber, W. R., Kish, J. C., & Rockstroh, J. M. 1973, Proc. 13th Int. Cosmic-Ray Conf. (Denver), 2, 760